Proceedings of the Korean Nuclear Society Autumn Meeting
Yongpyong, Korea, 2003

Semi-Analog Monte Carlo (SMC) Method for Time-Dependent Three-Dimensional Heterogeneous Radiative Transfer Problems

SungHwan Yun and Nam Zin Cho

Korea Advanced Institute of Science and Technology
373-1 Kusong-dong, Yusong-gu
Taejon, Korea, 305-701

ABSTRACT

Radiative tranfer is a complex phenomenon in which radiation field interacts with material. This time-dependent non-linear radiative transfer problem can be solved by Monte Carlo method. However, due to huge computing time, there have been many efforts to reduce this computing time. As a result of this effort, several new methods were suggested. Semi-Analog Monte Carlo (SMC) method is very accurate regardless of the time step size used.

In this paper we extended this SMC method to solve 3-dimensional heterogeneous problems and computerized in a computer code. It was tested by applying it to a 1-D problem with analytic solution and to a heterogeneous 3-dimensional problem.

I. INTRODUCTION

The thermal radiative transfer equation describes the transport of photons in a medium. Up to now, there are many methods to solve time-dependent non-linear radiative transfer problems. The Implicit Monte Carlo (IMC) method developed by Fleck and Cummings [5] has been used for a long time until now. Although IMC is accurate in small time step, it needs huge computation time. Recently several new methods [6][9][10][11] were suggested to overcome time step dependency in IMC. Each method has both merit and demerit [7], but it is known that semi-analog Monte

Carlo (SMC) method developed by Ahrens and Larsen [6] is accurate regardless of the time step size. But the SMC method was developed for only 3-dimensional homogeneous problems. [7]

In this study, we extended the SMC method to 3-dimensional heterogeneous problems. The principal algorithm is as follows. Photons are born and then stream by random 3-dimensional direction to collision sites, where they are randomly scattered or absorbed by the material. If a photon is absorbed, its energy remains at the absorption site until the re-emission time, which is random. The absorbed photon increases the material energy.

II. DESCRIPTION OF SEMI-ANALOG MONTE CARLO (SMC) METHOD

Assuming Local Thermodynamic Equilibrium (LTE), which means that the matter is in thermal equilibrium at a temperature T and the photons emit in a Planckian Spectrum, and no scattering, the radiative transfer and material energy equations are[1]

$$\frac{1}{c}\frac{\partial I(r,\nu,\Omega,t)}{\partial t}+\Omega\cdot\nabla I(r,\nu,\Omega,t)=\sigma(r,\nu,T)\left[B(\nu,T)-I(r,\nu,\Omega,t)\right], \tag{1a}$$

$$\frac{\partial u_m(r,T)}{\partial t}=\int_{4\pi}\int_0^\infty \sigma(r,\nu,T)\left(I(r,\nu,\Omega,t)-B(\nu,T)\right)d\nu d\Omega+S(r,\nu,t), \tag{1b}$$

where the functions,

$$\mathbf{u_m(r,T)}: \quad \textbf{material energy density,} \tag{2a}$$

$$\mathbf{T(r,t)}: \quad \textbf{material temperature,} \tag{2b}$$

$$S(r,\nu,t): \quad \textbf{external isotropic photon source,} \tag{2c}$$

$$I(r,\nu,\Omega,t): \quad \textbf{specific photon intensity,} \tag{2d}$$

$$\sigma(r,\nu,T): \quad \textbf{opacity,} \tag{2e}$$

$$B(\nu,T)=\frac{2h}{c^2}\frac{\nu^3}{e^{h\nu/kT}-1}: \quad \textbf{Plank function.} \tag{2f}$$

In Eq. (1a), $I(r,\nu,\Omega,t)$ and $\sigma(r,\nu,T)$ correspond to the angular flux, $\psi(r,E,\Omega,t)$ and the total cross-section $\sigma(r,E,T)$ in neutronics. In Eq. (1b), $\mathbf{u_m(r,T)}$ may be viewed as the delayed neutron precursor $\mathbf{C_d(r,t)}$. However, owing to the nonlinear relationship between $\mathbf{u_m(r,T)}$ and $B(\nu,T)$, Eq. (1b) requires a special non-linearity treatment.

The other term to make the non-linearity in Eq. (1b) is the temperature dependent opacity $\sigma(r,\nu,T)$. Hence, for the special case of a frequency-independent opacity, $\sigma(r,\nu,T)$ is assumed as $\sigma(r)$.

The Plank function integrated over frequency (or energy) is

$$\int_0^\infty B(\nu,T)d\nu = \frac{ca}{4\pi}\left(T(r,t)\right)^4 , \tag{3}$$

where the radiation constant a is $\dfrac{8k^4\pi^5}{15c^3h^3}$.

Equilibrium radiation energy density is defined as follows:

$$u_r\left(r,T\right) \equiv a\left(T(r,t)\right)^4 . \tag{4}$$

Now frequency-integrated intensity and source are defined as follows:

$$\psi(r,\Omega,t) \equiv \int_0^\infty I(r,\nu,\Omega,t)d\nu , \tag{5}$$

$$s(r,t) \equiv \int_0^\infty S(r,\nu,t)d\nu . \tag{6}$$

Eqs. (1a) and (1b) can be integrated over frequency (grey approximation),

$$\frac{1}{c}\frac{\partial\psi(r,\Omega,t)}{\partial t} + \Omega\cdot\nabla\psi(r,\Omega,t) = \sigma(r)\left[\frac{cu_r\left(r,T\right)}{4\pi} - \psi(r,\Omega,t)\right], \tag{7a}$$

$$\frac{\partial u_m\left(r,T\right)}{\partial t} = \sigma(r)\left(\int_{4\pi}\psi(r,\Omega,t)d\Omega - \int_{4\pi}\frac{cu_r\left(r,T\right)}{4\pi}d\Omega\right) + s(r,t). \tag{7b}$$

Heat capacity C_V is defined as follows[2]:

$$\frac{\partial u_m\left(r,T\right)}{\partial T} = C_V(r,T). \tag{8}$$

The nonlinear relationship between $\mathbf{u_m(r,T)}$ and $\mathbf{u_r(r,T)}$ is

$$\begin{aligned}\frac{\partial u_m\left(r,T\right)}{\partial t} &= \frac{\partial u_r\left(r,T\right)}{\partial t}\frac{\partial u_m\left(r,T\right)}{\partial u_r\left(r,T\right)} \\ &= \frac{\partial u_r\left(r,T\right)}{\partial t}\frac{\partial T}{\partial u_r\left(r,T\right)}\frac{\partial u_m\left(r,T\right)}{\partial T} = \frac{C_V(r,T)}{4aT^3}\frac{\partial u_r\left(r,T\right)}{\partial t} \\ &= \frac{1}{\beta(r)}\frac{\partial u_r\left(r,T\right)}{\partial t},\end{aligned} \tag{9}$$

where $\beta(r)$, a dimensionless function, is defined as follows[6]:

$$\beta(r) = \frac{4aT^3}{C_V(r,T)} . \tag{10}$$

When the temperature is low, the heat capacity C_V becomes [2,12]

$$C_V(r,T) = C_V(r)T^3 . \tag{11}$$

Then $\beta(r)$ at low temperature becomes,

$$\beta(r) = \frac{4aT^3}{C_V(r)T^3} = \frac{4a}{C_V(r)} . \tag{12}$$

Therefore, this approximation of the nonlinear relationship between $\mathbf{u_m(r,T)}$ and $\mathbf{u_r(r,T)}$ is exact at low temperature.

Eq. (9) is substituted in Eq. (7b),

$$\frac{1}{\beta(r)}\frac{\partial u_r(r,T)}{\partial t} = \sigma(r)\left(\int_{4\pi}\psi(r,\Omega,t)d\Omega - \int_{4\pi}\frac{cu_r(r,T)}{4\pi}d\Omega\right) + s(r,t). \tag{13}$$

Then, the analytic solution of Eq. (13) is,

$$\begin{aligned} u_r(r,T) = u_r^0(r)e^{-c\beta\sigma(r)t} + \beta(r)\int_0^t \sigma(r)e^{-c\beta(r)\sigma(r)(t-t')}\int_{4\pi}\psi(r,\Omega,t')d\Omega dt' \\ + \beta(r)\int_0^t e^{-c\beta(r)\sigma(r)(t-t')}s(r,t')dt', \end{aligned} \tag{14}$$

where $u_r^0(r)$ is equilibrium radiation energy density at initial time (t=0).

Eq. (14) is now substituted in Eq. (7a),

$$\begin{aligned} &\frac{1}{c}\frac{\partial\psi(r,\Omega,t)}{\partial t} + \Omega\cdot\nabla\psi(r,\Omega,t) - \sigma(r)\psi(r,\Omega,t) = \\ &\frac{c\sigma(r)}{4\pi}u_r^0(r)e^{-c\beta\sigma(r)t} + \frac{c\sigma(r)}{4\pi}\beta\int_0^t\sigma(r)e^{-c\beta\sigma(r)(t-t')}\int_{4\pi}\psi(r,\Omega,t')d\Omega dt' \\ &+ \frac{c\sigma(r)}{4\pi}\beta\int_0^t e^{-c\beta\sigma(r)(t-t')}s(r,t')dt'. \end{aligned} \tag{15}$$

The first term in R.H.S. of Eq. (15) represents the emission due to the initial temperature distribution $u_r^0(r)$ and the second term represents emissions as a result of temperature changes since the initial time $t=0$ and the third term represents emissions as a result of external source since the initial time $t=0$.

In the first term, the particle emission times are sampled from an exponential PDF,

$$\xi_m = e^{-c\beta(r)\sigma t}, \tag{16a}$$

or

$$t = -\frac{1}{c\beta(r)\sigma}\ln[\xi_m], \tag{16b}$$

where ξ_m is the random number between 0 and 1.

In the second and third terms, for a collision at time t', the contribution of emitted particles at time t has a distribution of $e^{-c\beta\sigma(r)(t-t')}$. Then the particle emission times are sampled from an exponential PDF,

$$\int_{t'}^{t} d\tilde{t}\, c\sigma\beta e^{-c\beta\sigma(\tilde{t}-t')} = \xi_m, \tag{17a}$$

or

$$t = t' - \frac{1}{c\beta\sigma}\ln[\xi_m]. \tag{17b}$$

Eq. (15) can be solved by Monte Carlo method as in a neutron transport problem. The flow chart of the whole calculation is shown in < Fig. 1. >. Especially, the flow chart of heterogeneous calculation is shown in < Fig. 2. >. In 3 dimensional heterogeneous calculations, the distance of particle flight, s is determined as follows:

$$s = \sum_{j=1}^{l-1} s_j - \frac{\sum_{j=1}^{l-1}\sigma_j s_j + \ln\xi_d}{\sigma_l}, \tag{18}$$

where j is the mesh number where particle passes and l is the mesh number where particle collides.

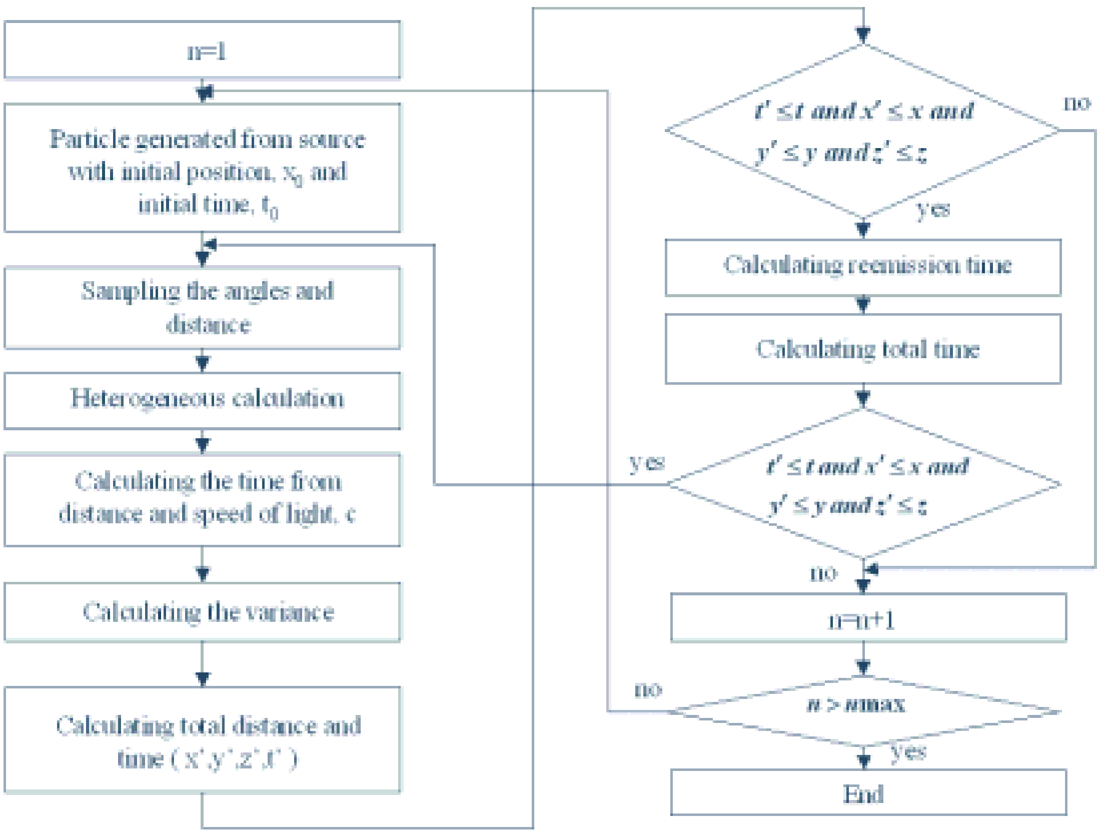

< Fig.1. Flowchart of 3-D SMC Calculation >

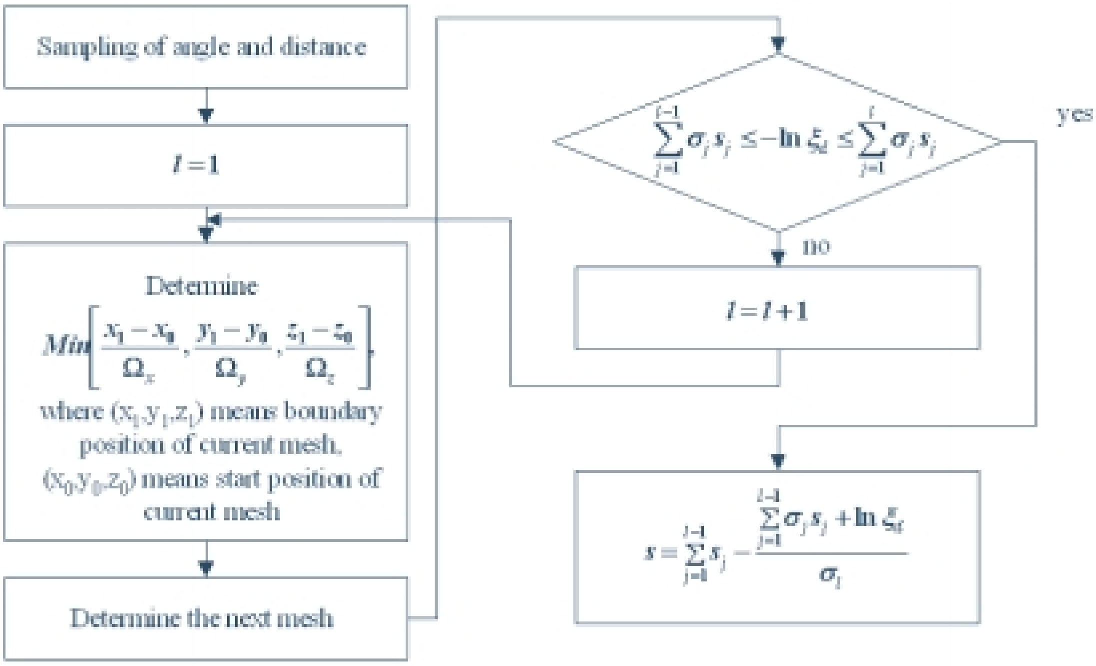

< Fig.2. Flowchart of Heterogeneous Calculation >

III. NUMERICAL RESULTS

The code uses an XYZ mesh with mesh spacing, with material properties assumed constant within each mesh cell for the duration of a time step. There is no time discretization for tallies. Each time step is only for observation of the results.

The first test problem is Su-Olson Benchmark Problem. [8] The problem consists of an infinite, homogeneous slab with a unit radiation source in $-0.5 < x < 0.5$ (in mean free path $[\,1/\sigma\,]$) and it is assumed initially cold (which means $u_r^0(r)$, the initial radiation density is 0.) for times $0 < t < 10$ (in mean free time $[\,1/c\sigma\beta\,]$), with the constants $c = \beta = \sigma = 1.0$ for non-dimensionalization. Analytic solutions are provided based on the transport equation for time, 1, 10 and 31.6 mft.

The mesh size used in calculation of SMC is 0.01 for $0 < x < 0.05$ and 0.1 for $0.05 < x < 10.0$ and 10.0 for y and z. The calculation is performed with $0 < x < 10$, $0 < y < 10$ and $0 < z < 10$ with the reflective boundary conditions at the x=0 plan, y=0 plan, z=0 plan, y=10 plan and z=10 plan. At the x=10 plan, the vacuum boundary condition is used.

Relative error R is used for statistical precision with respect to the estimated mean.

$$R \equiv \frac{\sigma(\hat{x})}{\hat{x}} = \frac{\sigma(x)}{\sqrt{N}\,\hat{x}}, \tag{19}$$

where

$$\hat{x} = \frac{1}{N}\sum_{i=1}^{N} x_i \quad : \quad \textbf{sample mean,} \tag{20a}$$

$$\sigma^2(x) == \frac{1}{N}\sum_{i=1}^{N} x_i^2 - \left(\frac{1}{N}\sum_{i=1}^{N} x_i\right)^2 \quad : \quad \textbf{sample standard deviation,} \tag{20b}$$

$$\sigma(\hat{x}) = \frac{\sigma(x)}{\sqrt{N}}. \quad : \quad \textbf{the variance of sample mean.} \tag{20c}$$

The results of the first test problem is shown in < Fig. 3. > . The relative error of this problem is shown in < Fig. 4 > .The results of parallel computation are shown in < Table 1 > and < Fig. 5 >.

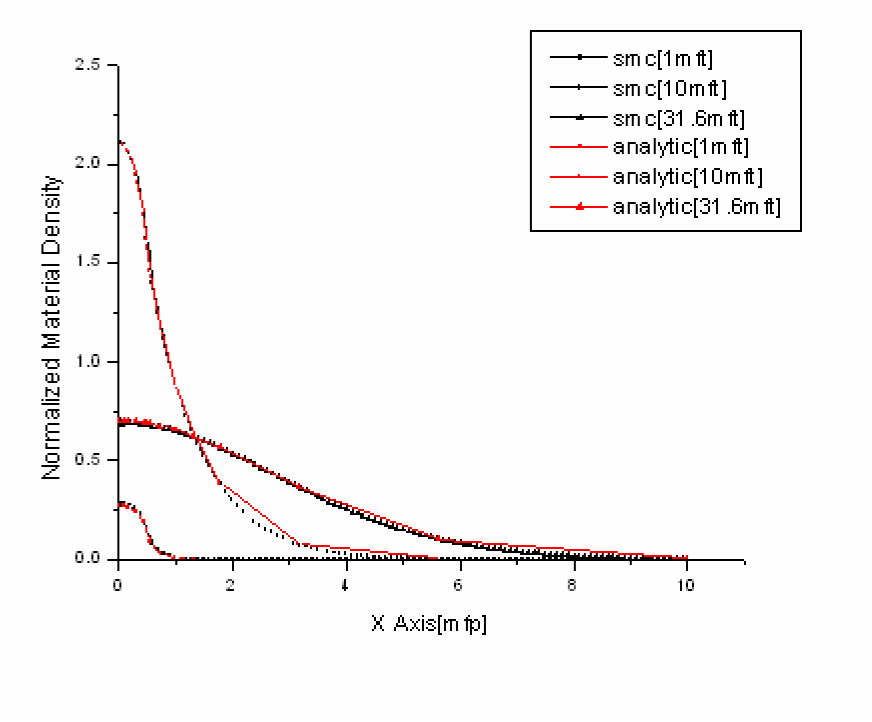

< Fig.3. Material energy density in the first test problem with 10^7 histories>

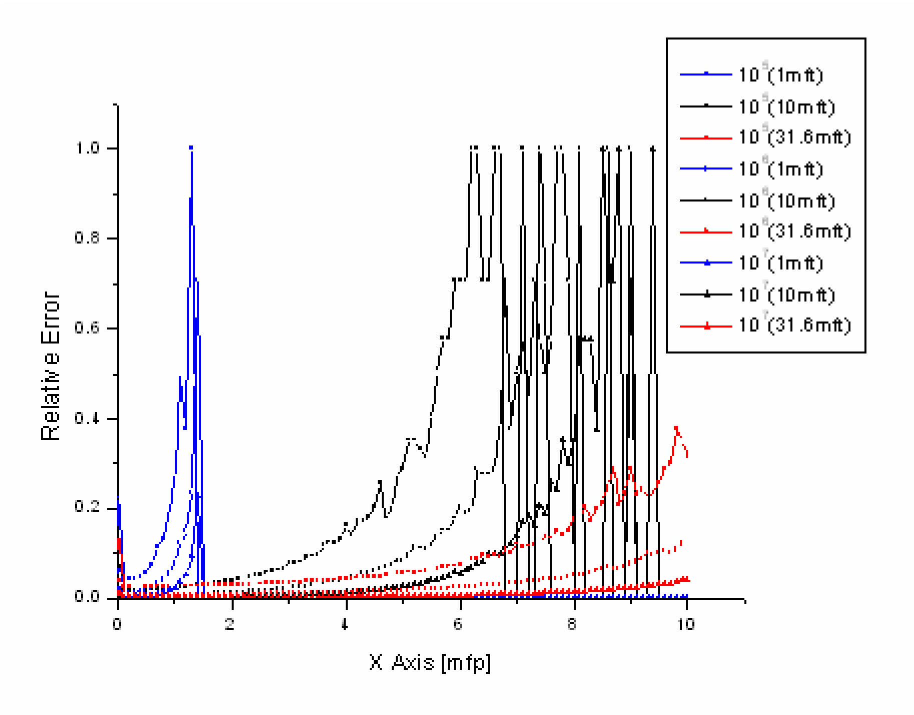

< Fig.4. Relative Error in the first test problem >

< Table 1. Results of Parallel Computation>

Number of CPUs	Computing Time	Speedup
1	1153.81	1
2	577.90	1.997
5	231.78	4.978
8	146.87	7.856
10	117.39	9.829
20	63.21	18.254

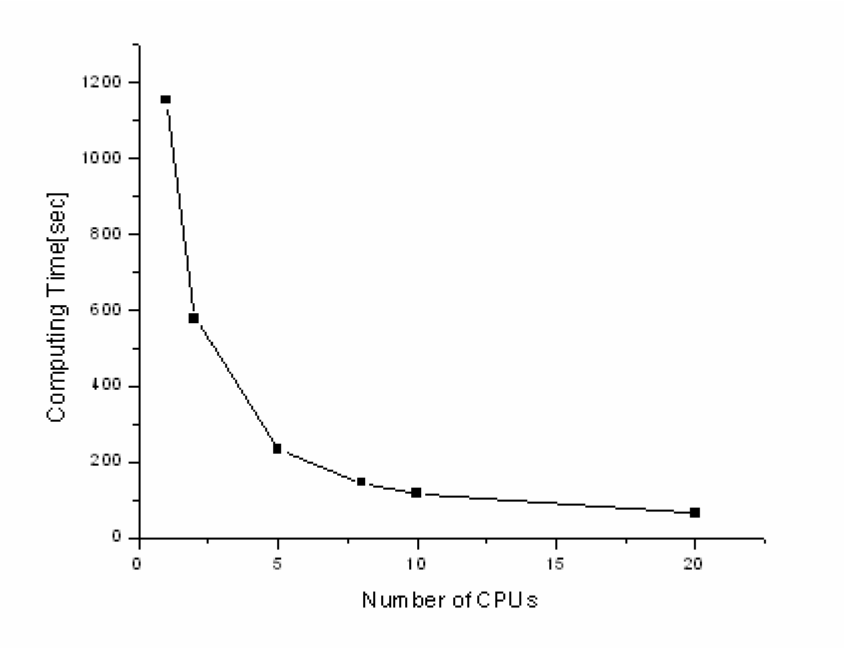

< Fig. 5. Computing time of Parallel Computation >

The second test problem is defined in < Table 2 > and < Fig.6 >. The information of materials and opacities is in < Table 3 > and < Table 4 >. We assume that all photons are of energy 1MeV. In < Table 3 >, the heat capacities are obtained as follows:[2]

$$\boldsymbol{C}_{\mathrm{v}}(\mathbf{r}) = \frac{\mathbf{12}\pi^{4}}{\mathbf{5}}\mathbf{R}\left(\frac{\mathbf{1}}{\theta_{\mathrm{D}}}\right)^{3}, \tag{21}$$

where

$$\theta_D \ \left[\mathbf{K}^{\circ}\right]: \textbf{the Debye temperature},$$

$$\boldsymbol{R} = \mathbf{8.3143} \times \mathbf{10}^{3}\left[\mathbf{J}\big/\mathbf{kmole}\cdot\mathbf{K}^{\circ}\right]: \textbf{the universal gas constant}.$$

The radiation coefficient $\boldsymbol{a}$ is used as the best experimental value of the Stefan-Boltzmann constant:[2]

$$\begin{aligned} \boldsymbol{a} &= \mathbf{7.561} \times \mathbf{10}^{-16}\left[\mathbf{J}\big/\mathbf{m}^{3}\boldsymbol{K}^{\circ 4}\right] \\ &= \mathbf{7.561} \times \mathbf{10}^{-22}\left[\mathbf{J}\big/\mathbf{cm}^{3}\boldsymbol{K}^{\circ 4}\right]. \end{aligned} \tag{22}$$

The source exists only in region 1 from $\boldsymbol{t} = \mathbf{0}\,[\mathbf{sec}]$ to $\boldsymbol{t} = \mathbf{100}\,[\mathbf{sec}]$ with uniform distribution of intensity $\mathbf{10}^{6}\left[\boldsymbol{MeV}\big/\mathbf{sec}\cdot\boldsymbol{cm}^{3}\right]$. The mesh size used in the calculation is 0.2$[\boldsymbol{cm}]$ in all x, y and z directions and $\mathbf{3}\times\mathbf{10}^{8}$ histories are used. The results of the second test problem are shown in < Fig. 7 > , < Fig. 8>, < Fig. 9 > and < Fig. 10 >.

< Table 2. Configuration of the second test problem >

Region	Length $[cm]$	Material
1	$-2.0 < x < 2.0$ $-2.0 < y < 2.0$ $-2.0 < z < 2.0$	Aluminum (Al)
2	$-6.0 < x < -2.0$, $2.0 < x < 6.0$ $-6.0 < y < -2.0$, $2.0 < y < 6.0$ $-6.0 < z < -2.0$, $2.0 < z < 6.0$	Copper (Cu)
3	$-12.0 < x < -6.0$, $6.0 < x < 12.0$ $-12.0 < y < -6.0$, $6.0 < y < 12.0$ $-12.0 < z < -6.0$, $6.0 < z < 12.0$	Carbon (C)
-	$x < -12.0$, $12.0 < x$ $y < -12.0$, $12.0 < y$ $z < -12.0$, $12.0 < z$	Vacuum

< Table 3. Information of materials in the second test problem > [2]

Material	Gas constant (R) $[J/g \cdot K^{\circ}]$	Debye temperature (θ_D) $[K^{\circ}]$	Heat Capacity $(C_v)[J/cm^3 \cdot K^{\circ 4}]$	$\beta(r) = \dfrac{4a}{C_V(r)}$
Aluminum (Al)	0.639538	398	$\mathbf{6.40312 \times 10^{-6}}$	$\mathbf{4.72332 \times 10^{-16}}$
Copper (Cu)	0.28669	315	$\mathbf{1.91918 \times 10^{-5}}$	$\mathbf{1.57589 \times 10^{-16}}$
Carbon (C)	1.385667	1860	$\mathbf{1.14276 \times 10^{-7}}$	$\mathbf{2.64657 \times 10^{-14}}$

< Table 4. The opacities of materials in the second test problem > [14]

Material	Total Opacity at 1MeV $[cm^{-1}]$	Absorption Opacity at 1MeV $[cm^{-1}]$
Aluminum (Al)	0.54953	0.24165
Copper (Cu)	0.132795	0.05902
Carbon (C)	0.17172	0.07803

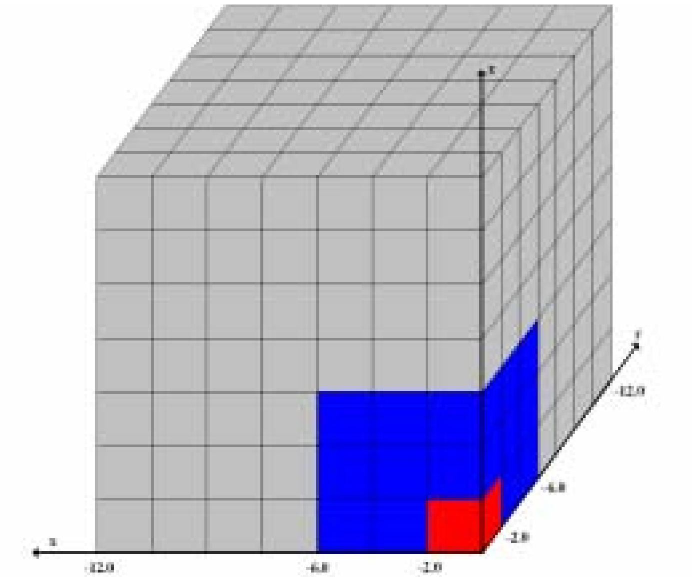

< Fig. 6. Configuration of the second problem in $(x < 0,\ y < 0,\ z > 0)$ octant >

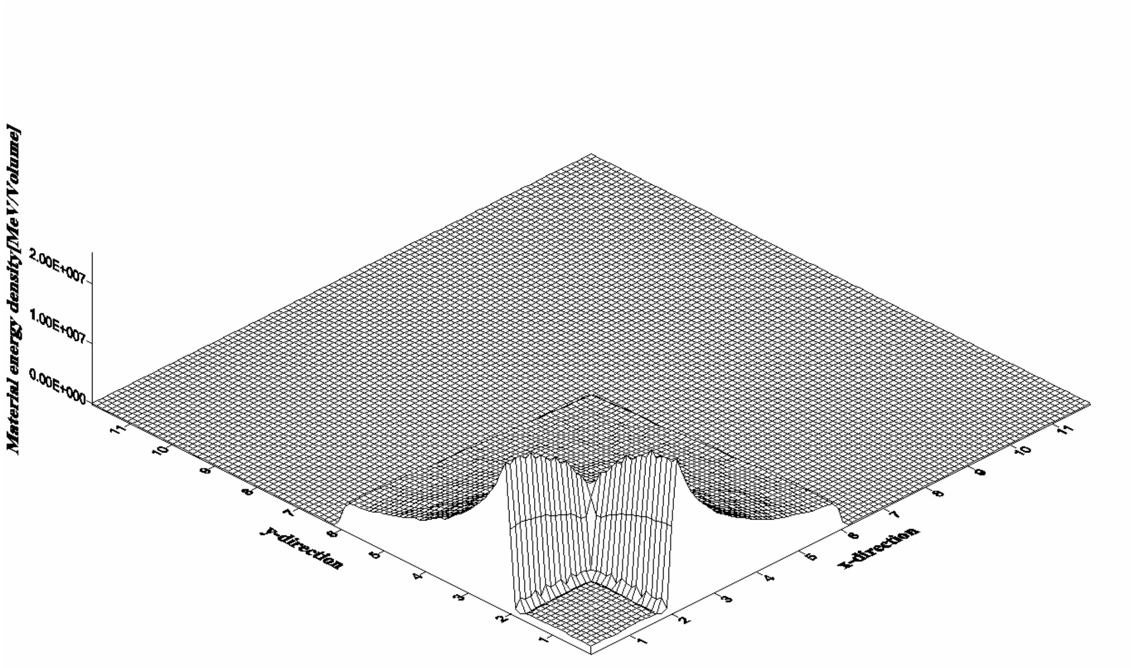

< Fig. 7. The results of the second problem at $(z,t) = (1\,cm\ ,\ 1.5\times10^{6}\ \sec)$ >

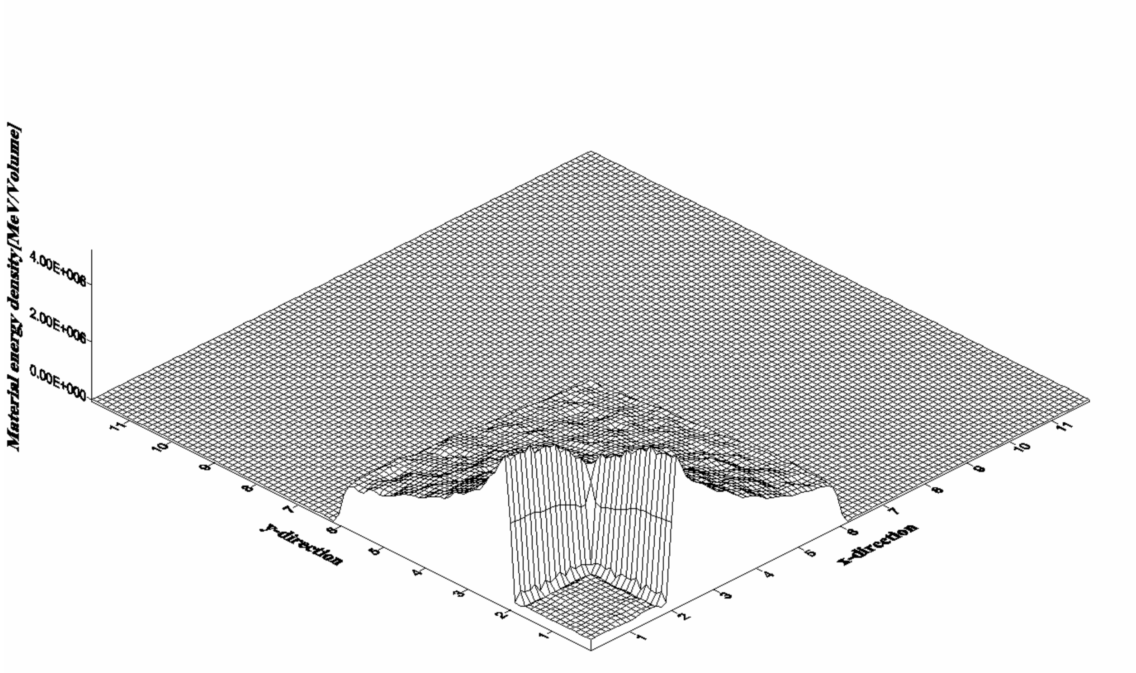

< Fig. 8. The results of the second problem at $(z,t) = (1\,cm\,,\,3\times10^{6}\ \text{sec})$ >

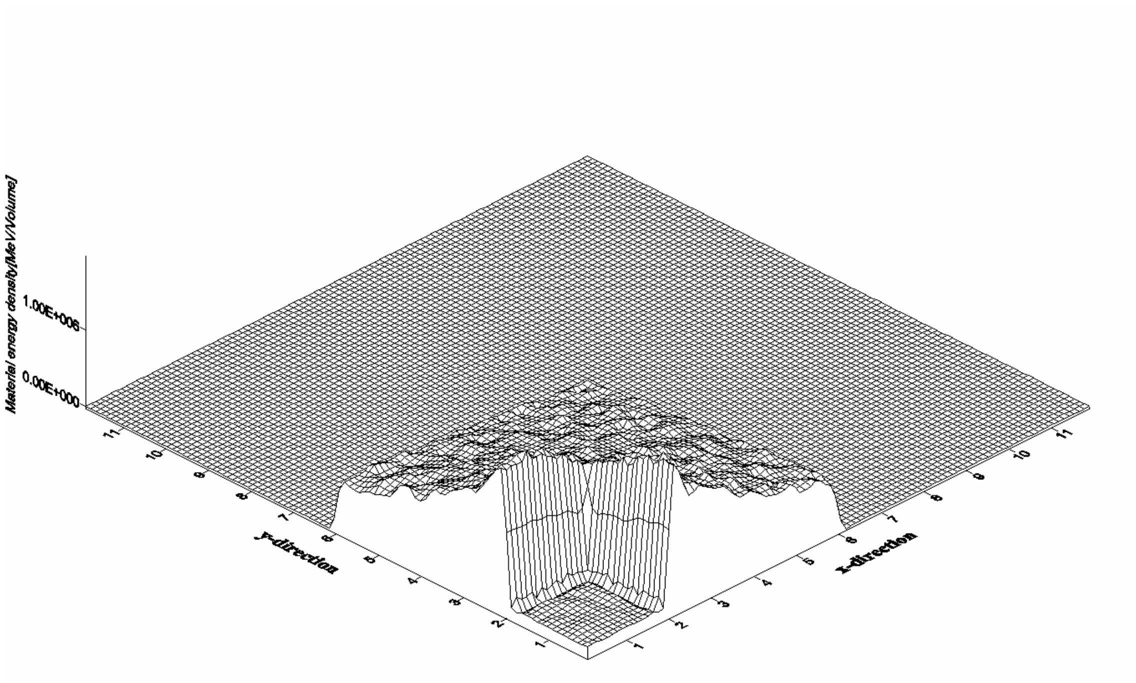

< Fig. 9. The results of the second problem at $(z,t) = (1\,cm\,,\,4\times10^{6}\ \text{sec})$ >

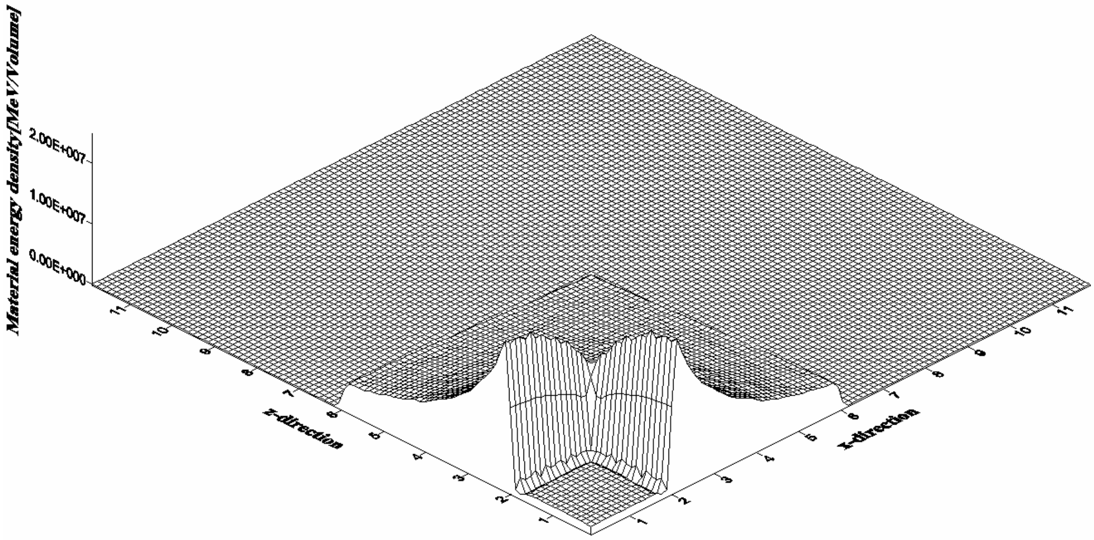

< Fig. 10. The results of the second problem at $(y,t) = (1\,cm\,, 1.5\times10^{6}\ \sec)$ >

IV. CONCLUSIONS

The 3-dimensional heterogeneous semi-analog Monte Carlo (SMC) method was developed and computerized in a computer code to solve time-dependent non-linear radiative transfer problems. It was tested on a 1-dimensional test problem and the results are accurate comparing with the available analytic solutions. The 3-dimensional heterogeneous problem was also solved.

To reduce computation time, the parallel computation is used and shows good performance.

ACKNOWLEDGEMENT

This work was supported in part by the Ministry of Science and Technology of Korea through the National Research Laboratory (NRL) Program.

REFERENCES

1. G. C. Pomraning, “The Equations of Radiation Hydrodynamics,” Pergamon Press, Oxford, 1793.
2. F. Sears and G. Salinger, Thermodynamics, Kinetic Theory, and Statistical Thermodynamics, Addison-Wesley, 1975.
3. Malvin H. Kalos and Paula A. Whitlock, “Monte Carlo Methods,” John Wiley & Sons, 1986.
4. E.E. Lewis and W.F. Miller, Jr. Computational Methods of Neutron Transport, John Wiley & Sons, New York, 1984.
5. J. A. Fleck, Jr and J. D. Cummings “An Implicit Monte Carlo Scheme for Calculating Time and Frequency Dependent Nonlinear Radiation Transport,” *J.Comp.Phys*.,**8**,313,1971.
6. Cory Ahrens and Edward W. Larsen “A Semi-analog Monte Carlo Method for Grey Radiative Transfer Problems,” *Proceedings ANS Mathematics and Computations Topical Meeting*, Salt Lake City, Sept 2001.
7. W. R. Martin and F. B. Brown, “Comparison of Monte Carlo Methods for Nonlinear Radiation Transport,” *Proceedings ANS Mathematics and Computations Topical Meeting*, Salt Lake City, Sept 2001.
8. B. Su and G. L. Olson, “An Analytical Benchmark for Non-Equilibrium Radiative Transfer in an Isotropically Scattering Medium,” *Ann. Nucl. Energy.*, 24, 13, 1997.
9. W. R. Martin and F. B. Brown, “The Analytical Monte Carlo Method for Radiation Transport Calculations,” *Trans. Am. Nucl. Soc.*, **84**, 217, June 2001.
10. F. B. Brown and W. R. Martin, “Monte Carlo Particle Transport in Media with Exponentially Varying Time-Dependent Cross Sections,” *Trans. Am. Nucl. Soc.*, **84**, 220, June 2001.
11. F. B. Brown and W. R. Martin, “Improved Method for Implicit Monte Carlo,” *Trans. Am. Nucl. Soc.*, **87**, 212, Nov 2002.
12. H. Y. Kim, “Investigation of Monte Carlo Methods for Time-Dependent Nonlinear Radiative Transfer Problems,” M. S. thesis, KAIST, 2003.
13. Stephen A. Dupree and Stanley K. Fraley, “A Monte Carlo Primer, A Practical Approach to Radiation Transport,” Kluwer Academic/Plenum Publishers, 2002.
14. John R. Lamarsh, “Introduction to Nuclear Engineering,” Prentice Hall, 2001.